

**UTILIZATION OF METHANE: METHYLATION OF BENZENE WITH
METHANE AND GAS-TO-LIQUIDS (GTL) VIA FISCHER-TROPSCH
SYNTHESIS**

Thani Jermwongratanachai

A Dissertation Submitted in Partial Fulfillment of the Requirements
for the Degree of Doctor of Philosophy
The Petroleum and Petrochemical College, Chulalongkorn University
in Academic Partnership with
The University of Michigan, The University of Oklahoma,
and Case Western Reserve University

2014

T28370569

Thesis Title: Utilization of Methane: Methylation of Benzene with Methane and Gas-to-Liquids (GTL) via Fischer-Tropsch Synthesis

By: Thani Jermwongratanachai


Program: Petrochemical Technology

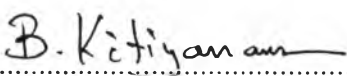
Thesis Advisors: Asst. Prof. Boonyarach Kitiyanan
Prof. Burtron H. Davis
Dr. Gary Jacobs


Accepted by The Petroleum and Petrochemical College, Chulalongkorn University, in partial fulfilment of the requirements for the Degree of Doctor of Philosophy.

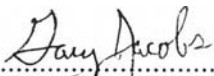

..... College Dean
(Asst. Prof. Pomthong Malakul)

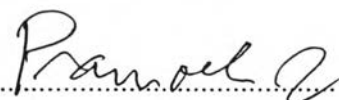
Thesis Committee:

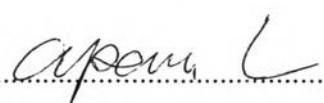

.....
(Asst. Prof. Pomthong Malakul)


.....
(Asst. Prof. Boonyarach Kitiyanan)


.....
(Prof. Burtron H. Davis)


.....
(Dr. Gary Jacobs)


.....
(Assoc. Prof. Pramoch Rangsunvigit)


.....
(Assoc. Prof. Apanee Luengnaruemitchai)


.....
(Dr. Tanate Danuthai)

ABSTRACT

5281004063: Petrochemical Technology Program

Thani Jermwongratanachai: Utilization of Methane: Methylation of Benzene with Methane and Gas-to-Liquids (GTL) via Fischer-Tropsch Synthesis.

Thesis Advisors: Asst. Prof. Boonyarach Kitiyanan, Prof. Burtron H. Davis, and Dr. Gary Jacobs 235 pp.

Keywords: Methylation/ Benzene/ Methane/ HZSM-5/ Gas-to-liquids (GTL)/ Fischer-Tropsch synthesis/ Cobalt (Co)/ Alumina (Al_2O_3)

During the past decades, studies on the conversion of methane, a main component of natural gas, into more valuable fuels or chemicals have received much attention. This is because liquid-petroleum reserves are becoming scarcer, while natural gas (e.g., methane) reserves are abundant; moreover, methane can be generated by fermentation of organic materials. Previously, methane was predominantly used for heating, in both industry and in households. Once the gas-to-liquids (GTL) technology for the conversion of methane into higher valued liquid products (e.g., gasoline, diesel, and methanol) was accomplished, it has largely inspired many researchers to widen research in this area by either developing a new approach of utilizing methane or improving the performance of existing technologies. In this thesis, the work is divided into two parts. First, methylation of benzene with methane, a novel and challenging approach is aimed at directly using methane as an alkylating agent to react with the benzene ring into methylated product, especially xylenes, in a one-step process. Ag/HZSM-5 and Mo/HZSM-5 were studied as catalysts. The second study was on the heart of GTL technology, Fischer-Tropsch synthesis, a reaction to produce long chain hydrocarbons, which can be hydrocracked to produce gasoline, diesel, jet fuels, and waxes, from synthesis gas derived from methane/natural gas. The capability of some transition metals as metal promoters for Co/ Al_2O_3 Fischer-Tropsch catalyst was demonstrated. Moreover, reoxidation of tiny cobalt crystallite at the onset of the reaction was explored and proposed as one of the modes of catalyst deactivation for very small nanocrystallites.

บทคัดย่อ

ธานี เจริญวงศ์รัตนชัย : การใช้ประโยชน์จากก๊าซมีเทนด้วยวิธีการเติมหมู่เมทิลบนสารเบนซีนโดยใช้ก๊าซมีเทนและการเปลี่ยนก๊าซมีเทนให้เป็นสารไฮโดรคาร์บอนในสถานะของเหลวโดยใช้ปฏิกิริยาสังเคราะห์ฟิชเชอร์-โทรปช์ (Utilization of Methane: Methylation of Benzene with Methane and Gas-to-Liquids (GTL) via Fischer-Tropsch Synthesis) อาจารย์ที่ปรึกษา : ผศ. ดร. บุญยรัชต์ กิตติยานันท์ ศ. ดร. เบอดัน เดวิส และ ดร. แกรี จาคอบส์ 235 หน้า

ในช่วงระยะเวลาสิบปีที่ผ่านมา มีการศึกษาการเปลี่ยนก๊าซมีเทนไปเป็นน้ำมันเชื้อเพลิงและสารเคมีชนิดอื่นที่มีมูลค่าสูงขึ้นกันอย่างกว้างขวาง เนื่องจากแหล่งน้ำมันดิบเริ่มมีปริมาณลดลง ในขณะที่แหล่งก๊าซธรรมชาติซึ่งมีก๊าซมีเทนเป็นองค์ประกอบหลักยังมีในปริมาณมากและก๊าซมีเทนยังสามารถผลิตได้จากกระบวนการหมักสารอินทรีย์ ในอดีตก๊าซมีเทนถูกใช้เพื่อเป็นสารเชื้อเพลิงในภาคอุตสาหกรรมและภาคครัวเรือนเป็นหลัก นับตั้งแต่เทคโนโลยีการเปลี่ยนก๊าซเป็นของเหลว (Gas-to-Liquids (GTL) technology) ได้ถูกพัฒนาขึ้น จึงเริ่มมีการตื่นตัวในการศึกษาวิจัยการเพิ่มมูลค่าก๊าซมีเทนกันมากขึ้น ทั้งการคิดค้นเทคโนโลยีใหม่เพื่อเพิ่มมูลค่าก๊าซมีเทนและการพัฒนาปรับปรุงประสิทธิภาพเทคโนโลยีเดิม ตัวอย่างเช่น เทคโนโลยีฟิชเชอร์-โทรปช์ โดยในงานวิจัยนี้ผู้วิจัยได้ทำการศึกษาวิจัยในสองแนวทางดังกล่าว ได้แก่ 1. การคิดค้นเทคโนโลยีใหม่โดยศึกษาปฏิกิริยาการเติมหมู่เมทิลบนวงแหวนเบนซีนโดยใช้ก๊าซมีเทน (Methylation of Benzene with Methane) เพื่อให้ได้สารเคมีที่มีมูลค่าสูง เช่น พาราไซลีน โดยงานวิจัยนี้ได้มุ่งเน้นไปที่การใช้ตัวเร่งปฏิกิริยาและการปรับสภาวะปฏิกิริยา 2. การวิจัยเพื่อพัฒนาประสิทธิภาพของตัวเร่งปฏิกิริยาสำหรับปฏิกิริยาสังเคราะห์ฟิชเชอร์-โทรปช์ (Fischer-Tropsch synthesis) ซึ่งเป็นปฏิกิริยาการผลิตสารไฮโดรคาร์บอนโซ่ยาวจากก๊าซสังเคราะห์ (synthesis gas) ที่ได้มาจากก๊าซมีเทน ในงานวิจัยได้ศึกษาการใช้โลหะแทรนซิชันเป็นสารเพิ่มประสิทธิภาพของตัวเร่งปฏิกิริยาชนิด โคบอลต์บนตัวรองรับอะลูมินา (Co/Al₂O₃) นอกจากนี้งานวิจัยยังได้เสนอสาเหตุของการเสื่อมประสิทธิภาพของตัวเร่งปฏิกิริยา ณ ขณะเริ่มต้นปฏิกิริยากันเนื่องมาจากปฏิกิริยาออกซิเดชันของโลหะโคบอลต์ที่มีขนาดเล็ก ซึ่งการค้นพบดังกล่าวนี้จะเป็นประโยชน์สำหรับการพัฒนาตัวเร่งปฏิกิริยาชนิดนี้ต่อไป

ACKNOWLEDGEMENTS

For the completion of this dissertation, I would like to sincerely acknowledge my advisor, Asst. Prof. Boonyarach Kitiyanan, for his exceptional supervision, knowledge, suggestion, helpfulness, and encouragement, in addition to an opportunity to experience challenging researches both in Thailand and USA. It has been a great pleasure working with him for the past four years.

My great honours and appreciations also go to Prof. Burtron H. Davis, Associate Director of Center for Applied Energy Research (CAER), University of Kentucky, USA, and Dr. Gary Jacobs, research engineer at this center, for providing me a priceless opportunity to study and perform research at this excellent center. I really appreciate their wonderful guidance, knowledge, and friendship during my one-year research at CAER. It has been a great pleasure working with them as well.

The author is grateful for the scholarship provided by the Thailand Research Fund through the Royal Golden Jubilee (RGJ) Ph.D. Program; The Petroleum and Petrochemical College (PPC); and The National Center of Excellence for Petroleum, Petrochemicals, and Advanced Materials, Thailand, moreover, the financial support from the PTT Global Chemical Company Limited (PTTGC). In addition, the author also appreciates Fulbright-Thailand Research Fund Junior Research Scholarship Program for all their helps during my grant period in the United State.

I would also like to express my appreciation to all the PPC faculties for providing the precious fundamental knowledge and to all PPC staffs for their great contributions throughout my five-year long study.

Special thanks go to all the PPC and CAER friends for their great friendship, creative guidance, helpfulness, and encouragement.

Finally, I would like to dedicate this dissertation to my parents and my family, who have understood, supported, and encouraged me during my five-year long study.

TABLE OF CONTENTS

	PAGE
Title Page	i
Abstract (in English)	iii
Abstract (in Thai)	iv
Acknowledgements	v
Table of Contents	vi
List of Tables	x
List of Figures	xii
Abbreviations	xxi
List of Symbols	xxiii
 CHAPTER	
I INTRODUCTION	1
II THEORETICAL BACKGROUND AND LITERATURE REVIEW	5
2.1 Methane	5
2.1.1 Source of Methane	5
2.1.2 Utilization	7
2.2 Aromatics and Alkylation Reaction	9
2.2.1 Production of Aromatics: the UOP Aromatics Complex Process	9
2.2.2 Alkylation of Aromatics	12
2.2.3 Methane as an Alkylating Agent	14
2.2.4 Methylation of Benzene with Methane and its Derivatives	18
2.3 Gas-to-liquids (GTL) Technology	24
2.3.1 Synthesis Gas Production from Natural Gas	25
2.3.2 Fischer-Tropsch Process	27

CHAPTER	PAGE
2.3.3 Product Upgrading	32
III THERMODYNAMICS CONSIDERATIONS	33
3.1 Definition of the Equilibrium Constant	33
3.2 Gibbs Free Energy of Reaction	34
3.3 Calculation of Equilibrium Conversion	35
IV EXPERIMENTAL	45
4.1 Materials	45
4.1.1 Materials	45
4.1.2 Gases	45
4.2 Experimental Procedures	46
4.2.1 Catalyst Preparation	46
4.2.2 Catalyst Characterization	47
4.2.3 Catalyst Activity Test	53
V DIRECT METHYLATION OF BENZENE WITH METHANE OVER Ag/HZSM-5 CATALYST	57
5.1 Abstract	57
5.2 Introduction	58
5.3 Experimental	60
5.4 Results and Discussion	62
5.5 Conclusion	78
5.6 Acknowledgements	79
5.7 References	79
VI DIRECT METHYLATION OF BENZENE WITH METHANE OVER Mo/HZSM-5 CATALYST	83
6.1 Abstract	83
6.2 Introduction	84

CHAPTER	PAGE
6.3 Experimental	85
6.4 Results and Discussion	88
6.5 Conclusion	107
6.6 Acknowledgements	107
6.7 References	107
VII FISCHER-TROPSCH SYNTHESIS: COMPARISONS BETWEEN Pt AND Ag PROMOTED Co/Al₂O₃ CATALYSTS FOR REDUCIBILITY, LOCAL ATOMIC STRUCTURE, AND CATALYTIC ACTIVITY	111
7.1 Abstract	111
7.2 Introduction	112
7.3 Experimental	114
7.4 Results and Discussion	121
7.5 Conclusion	152
7.6 Acknowledgements	153
7.7 References	153
VIII FISCHER-TROPSCH SYNTHESIS: TPR AND XANES ANALYSIS OF THE IMPACT OF SIMULATED REGENERATION CYCLES ON THE REDUCIBILITY OF Co/ALUMINA CATALYSTS WITH DIFFERENT PROMOTERS (Pt, Ru, Re, Ag, Au, Rh, Ir)	158
8.1 Abstract	158
8.2 Introduction	159
8.3 Experimental	161
8.4 Results and Discussion	164
8.5 Conclusion	177
8.6 Acknowledgements	178
8.7 References	178

CHAPTER	PAGE
IX FISCHER-TROPSCH SYNTHESIS: OXIDATION OF A FRACTION OF COBALT CRYSTALLITES IN RESEARCH CATALYSTS AT THE ONSET OF FT AT PARTIAL PRESSURE MIMICKING 50% CO CONVERSION	182
9.1 Abstract	182
9.2 Introduction	183
9.3 Experimental	187
9.4 Results and Discussion	191
9.5 Conclusion	207
9.6 Acknowledgements	207
9.7 References	208
X CONCLUSIONS AND RECOMMENDATIONS	212
10.1 Conclusions	212
10.2 Recommendations	214
REFERENCES	215
APPENDIX	229
CURRICULUM VITAE	233

LIST OF TABLES

TABLE		PAGE
CHAPTER III		
3.1	Thermodynamic properties of all relevant species	36
3.2	Thermodynamic properties of all relevant species	43
CHAPTER V		
5.1	Chemical composition, surface area, and pore properties of catalyst samples	64
5.2	Benzene conversion and product selectivity ^a	69
5.3	Benzene conversion and product selectivity of the reaction with no H ₂ co-feed and H ₂ co-feed ^a	72
5.4	Benzene conversion and product selectivity of the reaction over Ag/HZSM-5(H) catalyst in the presence of H ₂ co-feed with varying methane to benzene molar ratio ^a	74
5.5	Benzene conversion and product selectivity of the reaction over Ag/HZSM-5(H) catalyst in the presence of H ₂ co-feed with varying space velocity (WHSV) ^a	76
CHAPTER VII		
7.1	The results of BET surface area and porosity measurements, hydrogen chemisorption/pulse reoxidation, and X-ray diffraction of catalysts	123
7.2	Results of EXAFS fitting parameters for references acquired near the Pt L _{III} -edge. The fitting ranges were approximately $\Delta k = 3-12 \text{ \AA}^{-1}$ and $\Delta R = 1.6-2.83 \text{ \AA}$, $S_0^2 = 0.9$	139
7.3	Results of EXAFS fitting parameters for references acquired near the Ag K-edge. The fitting ranges were approximately $\Delta k = 2-10 \text{ \AA}^{-1}$ and $\Delta R = 1.5-3.1 \text{ \AA}$, $S_0^2 = 0.9$	147

TABLE	PAGE
7.4 Activity and selectivity of the Fischer-Tropsch synthesis reaction on unpromoted Co/Al ₂ O ₃ catalyst compared to Pt and Ag promoted Co/Al ₂ O ₃ catalysts ^a	151
CHAPTER VIII	
8.1 Elemental analysis results of fresh and RO3 treated samples of metal promoted 25%Co/Al ₂ O ₃ catalysts	165
8.2 Linear combination fittings of promoted 25%Co/Al ₂ O ₃ catalysts (i.e., before and after simulated regeneration cycles and re-activation) with Co ⁰ and CoO*	175
CHAPTER IX	
9.1 The results of BET surface area and porosity measurements and H ₂ chemisorption/O ₂ pulse reoxidation results of supports and catalysts	193
9.2 Results of EXAFS fitting for data acquired near the Co K-edge for catalyst after activation and at the onset of FTS. The fitting ranges were approximately $\Delta k = 2-14 \text{ \AA}^{-1}$ and $\Delta R = 1.25 - 2.7 \text{ \AA}$, $S_0^2 = 0.9$	206
APPENDIX	
A1 The response factor calculated from calibration curve of each substances	232

LIST OF FIGURES

FIGURE		PAGE
CHAPTER II		
2.1	Global natural gas reserves and share of work primary energy.	6
2.2	Several alternatives for methane conversion.	9
2.3	Simple aromatics complex.	10
2.4	Integrated UOP aromatics complex.	11
2.5	Product slate flexibility of UOP aromatics process.	12
2.6	Summary of catalytic activity of various metals loaded on HZSM-5 for methane activation and methylation of ethylene.	15
2.7	The mechanism of methylation of benzene with methane on Ag/H-ZSM-5.	20
2.8	An overview of natural gas utilization.	24
2.9	A block flow diagram of the gas-to-liquids (GTL) process.	25
CHAPTER III		
3.1	Conversion of benzene as a function of temperature at 8 different values of methane to benzene (M/B) feed molar ratio.	38
3.2	Equilibrium constants of all 6 reactions as a function of temperature.	40
3.3	Equilibrium constant of all 7 reactions as a function of temperature.	42

FIGURE		PAGE
CHAPTER IV		
4.1	The schematic flow diagram of catalyst testing instrument for methylation reaction.	54
4.2	The schematic flow diagram of catalyst testing instrument for Fischer-Tropsch reaction.	56
CHAPTER V		
5.1	Comparative X-ray diffraction patterns of HZSM-5 and Ag/HZSM-5.	63
5.2	(Left) FE-SEM image of Ag/HZSM-5, (Right) its corresponding EDX mapping of Ag element.	63
5.3	Normalized UV-Vis DRS spectra of Ag/HZSM-5 catalysts calcined under different atmospheres.	66
5.4	H ₂ -TPR profiles of Ag/HZSM-5 catalysts calcined under different atmospheres.	66
5.5	UV-Vis DRS spectra of fresh and spent catalysts: (Top) Ag/HZSM-5(N), (Middle) Ag/HZSM-5(H), and (Bottom) Ag/HZSM-5(O).	71
5.6	Comparative UV-Vis DRS spectra of fresh Ag/HZSM-5(H) and spent Ag/HZSM-5(H) underwent the reaction conditions with/without H ₂ co-feed.	73
5.7	Comparative UV-Vis DRS spectra of spent Ag/HZSM-5(H) catalysts run with different methane to benzene molar ratio.	75
5.8	Comparative UV-Vis DRS spectra of spent Ag/HZSM-5(H) catalysts run with different WHSV.	77

FIGURE	PAGE
CHAPTER VI	
6.1 XPS spectra of Mo/HZSM-5 catalysts at Mo3d region, including (a) freshly calcined Mo/HZSM-5, (b) red-Mo/HZSM-5 (after reduction in 5% H_2/N_2 at 550 °C for 0.5 h), (c) oxi-Mo/HZSM-5 (after oxidation in O_2 at 550 °C for 0.5 h), (d) car-Mo/HZSM-5 (after carburization in 10% N_2/CH_4 at 700 °C for 0.5 h).	90
6.2 XPS spectrum at C1s region of car-Mo/HZSM-5 catalyst (after carburization in 10% N_2/CH_4 at 700 °C for 0.5 h).	90
6.3 - H_2 -TPR profiles of freshly calcined Mo/HZSM-5 (solid line) and Mo/HZSM-5 reduced, moving up, at 350 °C for 30 min and at 550 °C for 30 min, respectively.	92
6.4 X-ray diffraction patterns, including (a) freshly calcined Mo/HZSM-5, (b) red-Mo/HZSM-5 (after reduction in 5% H_2/N_2 at 550 °C for 0.5 h), (c) oxi-Mo/HZSM-5 (after oxidation in O_2 at 550 °C for 0.5 h), (d) car-Mo/HZSM-5 (after carburization in 10% N_2/CH_4 at 700 °C for 0.5 h). HZSM-5 peaks are not indexed.	93
6.5 (A) Benzene conversions vs. TOS of red-Mo/ZSM-5 (solid line), oxi-Mo/ZSM-5 (dotted line), and car-Mo/HZSM-5 (dash line), (B) toluene selectivity vs. TOS, (C) heavier aromatics vs. TOS.	97
6.6 A comparative XPS spectra at Mo3d region between (solid line) fresh and (dashed line) spent (at TOS of 160 min) Mo/HZSM-5 catalyst, including (a) red-Mo/HZSM-5, (b) oxi-Mo/HZSM-5, and (c) car-Mo/HZSM-5.	99
6.7 A comparative XPS spectra at C1s region between (solid line) fresh and (dashed line) spent (at TOS of 160 min) Mo/HZSM-5 catalyst, including (a) red-Mo/HZSM-5, (b) oxi-Mo/HZSM-5; and (c) car-Mo/HZSM-5.	99

FIGURE	PAGE
6.8 Benzene conversion and product selectivity at TOS of 40 min as a function of percentage of H ₂ co-feed. Reaction conditions: red-Mo/HZSM-5(Mo/Al = 0.5), T = 550 °C, M/B ratio = 70, WHSV = 3.7 h ⁻¹ .	101
6.9 XPS spectra of spent Mo/HZSM-5 catalysts at Mo3d region, including (a) red-Mo/HZSM-5 without H ₂ co-feed, (b) red-Mo/HZSM-5 with 50% H ₂ co-feed, (c) red-Mo/HZSM-5 with 75% H ₂ co-feed.	101
6.10 XPS spectra of spent Mo/HZSM-5 catalysts at Cls region, including (a) red-Mo/HZSM-5 without H ₂ co-feed. (b) red-Mo/HZSM-5 with 50%H ₂ co-feed. (c) red-Mo/HZSM-5 with 75%H ₂ co-feed.	102
6.11 Benzene conversion and product selectivity at TOS of 40 min as a function of reaction temperature. Reaction conditions: red-Mo/HZSM-5(Mo/Al = 0.5), 75%H ₂ co-feed, M/B ratio = 70, WHSV = 3.7 h ⁻¹ .	103
6.12 Benzene conversion and product selectivity at TOS of 40 min as a function of Mo loading. Reaction conditions: red-Mo/HZSM-5, T = 550 °C, 75%H ₂ co-feed, M/B ratio = 70, WHSV = 3.7 h ⁻¹ .	104
6.13 TPD-NH ₃ profiles of (a) HZSM-5, (b) Mo/HZSM-5 with Mo/Al : 0.1, (c) Mo/HZSM-5 with Mo/Al : 0.5, (d) Mo/HZSM-5 with Mo/Al : 1.0.	104
6.14 Benzene conversion and product selectivity at TOS of 40 min as a function of methane to benzene feed molar ratio. Reaction conditions: red-Mo/HZSM-5 (Mo/Al : 0.7), T = 550 °C, 75%H ₂ co-feed, WHSV = 3.7 h ⁻¹ .	105

FIGURE	PAGE
6.15 Benzene conversion and product selectivity at TOS of 40 min as a function of WHSV. Reaction conditions: red-Mo/HZSM-5 (Mo/Al : 0.7), T = 550 °C, 75% H_2 co-feed, M/B ratio = 70.	106

CHAPTER VII

7.1 (A) TPR profiles of (a) unpromoted and Pt promoted 25%Co/Al ₂ O ₃ catalysts, including (b) 0.5%, (c) 1.0%, (d) 2.0%, (e) 3.0%, (f) 4.0%, and (g) 5.0% by weight Pt. (B) TPR profiles of (a) unpromoted and Ag promoted 25%Co/Al ₂ O ₃ catalysts, including (b) 0.276%, (c) 0.553%, (d) 1.11%, (e) 1.66%, (f) 2.21%, and (g) 2.76% by weight Ag, atomically equivalent to those of Pt, respectively.	125
7.2 (A) X-ray diffraction profiles of (a) unpromoted and Pt promoted 25%Co/Al ₂ O ₃ catalysts, including (b) 0.5%, (c) 1.0%, (d) 2.0%, (e) 3.0%, (f) 4.0%, and (g) 5.0% by weight Pt. (B) X-ray diffraction profiles of (a) unpromoted and Ag promoted 25%Co/Al ₂ O ₃ catalysts, including (b) 0.276%, (c) 0.553%, (d) 1.11%, (e) 1.66%, (f) 2.21%, and (g) 2.76% by weight Ag, atomically equivalent to those of Pt, respectively.	129
7.3 (A) Normalized XANES spectra at the Pt L _{III} -edge of Pt-25%Co/Al ₂ O ₃ catalysts (calcined and reduced) and Pt reference compounds; PtO, PtO ₂ , and Pt ⁰ . (B) (left) TPR-XANES spectra and (right) their corresponding linear combination fittings from reference spectra in Figure 7.3(A) of, moving down, 0.5%Pt-25%Co/Al ₂ O ₃ ; 2.0%Pt-25%Co/Al ₂ O ₃ ; and 5.0%Pt-25%Co/Al ₂ O ₃ . (C) Normalized XANES spectra at the Pt L _{III} -edge of Pt promoted Co/Al ₂ O ₃	

FIGURE

PAGE

catalysts with different loadings; (solid line) 0.5%Pt, (dotted line) 2.0%Pt, and (dashed line) 5.0%Pt, after TPR after cooling to ambient conditions.

133

- 7.4 (A) k^3 -Weighted EXAFS Fourier transform magnitude spectra of Pt promoted Co/Al₂O₃ catalysts and Pt reference compounds. (B) TPR-EXAFS k^3 -Weighted Fourier transform magnitude spectra of 5.0%Pt-25%Co/Al₂O₃, (C) k^3 -weighted EXAFS Fourier transform magnitude spectra of Pt-promoted catalysts after TPR after cooling to ambient conditions: (a) raw $k^3 \cdot \chi(k)$ vs. k data; (b) filtered $k^3 \cdot \chi(k)$ vs. k data (solid line) and resulting fitting (filled circles); (c) Fourier transform magnitude spectra (solid line), and first shell fitting (filled), moving downward, (I) 0.5%Pt-25%Co/Al₂O₃; (II) 1.0%Pt-25%Co/Al₂O₃; (III) 2.0%Pt-25%Co/Al₂O₃; (IV) 3.0%Pt-25%Co/Al₂O₃; (V) 4.0%Pt-25%Co/Al₂O₃; (VI) 5.0%Pt-25%Co/Al₂O₃. (D) k^3 -Weighted Fourier transform magnitude spectra after the TPR after the catalysts were cooled to ambient conditions, (a) 0.5%Pt-25%Co/Al₂O₃; (b) 1.0%Pt-25%Co/Al₂O₃; (c) 2.0%Pt-25%Co/Al₂O₃; (d) 3.0%Pt-25%Co/Al₂O₃; (e) 4.0%Pt-25%Co/Al₂O₃; (f) 5.0%Pt-25%Co/Al₂O₃.

138

- 7.5 (A) Normalized XANES spectra at the Ag K-edge of Ag-25%Co/Al₂O₃ catalysts (calcined and reduced) and Ag reference compounds; AgO, Ag₂O, and Ag⁰. (B) (left) TPR-XANES spectra and (right) their corresponding linear combination fittings from reference spectra in Figure 7.5 (A) of, moving down, 0.276%Ag-25%Co/Al₂O₃; 1.11%Ag-25%Co/Al₂O₃; and 2.76%Ag-25%Co/Al₂O₃. (C)

FIGURE	PAGE
<p>Normalized XANES spectra at the Ag K-edge of Ag promoted Co/Al₂O₃ catalysts with different loadings; (solid line) 0.276%Ag, (dotted line) 1.11%Ag, and (dashed line) 2.76%Ag, after TPR after cooling to ambient conditions.</p>	141
<p>7.6 (A) k^1-Weighted EXAFS Fourier transform magnitude spectra of Ag promoted Co/Al₂O₃ catalysts and Ag reference compounds (not to scale), (B) TPR-EXAFS k^1-Weighted Fourier transform magnitude spectra of 2.76%Ag-25%Co/Al₂O₃, (D) k^1-weighted EXAFS Fourier transform magnitude spectra of Ag-promoted catalysts after TPR after cooling to ambient conditions: (a) raw $k^1 \cdot \chi(k)$ vs. k data; (b) filtered $k^1 \cdot \chi(k)$ vs. k data (solid line) and resulting fitting (filled circles); (c) Fourier transform magnitude spectra (solid line), and first shell fitting (filled), moving downward, (I) 0.276%Ag-25%Co/Al₂O₃; (II) 0.553%Ag-25%Co/Al₂O₃; (III) 1.11%Ag-25%Co/Al₂O₃; (IV) 1.66%Ag-25%Co/Al₂O₃; (V) 2.21%Ag-25%Co/Al₂O₃; (VI) 2.76%Ag-25%Co/Al₂O₃. (C) k^1-Weighted Fourier transform magnitude spectra after the TPR after the catalysts were cooled to ambient conditions, (a) 0.276%Ag-25%Co/Al₂O₃; (b) 0.553%Ag-25%Co/Al₂O₃; (c) 1.11%Ag-25%Co/Al₂O₃; (d) 1.66%Ag-25%Co/Al₂O₃; (e) 2.21%Ag-25%Co/Al₂O₃; and (f) 2.76%Ag-25%Co/Al₂O₃.</p>	146

CHAPTER VIII

8.1	Comparative TPR spectra of unpromoted 25%Co/Al ₂ O ₃ catalysts before and after simulated regeneration cycles (e.g., 1 cycle (RO1), 2 cycles (RO2), and 3 cycles (RO3)).	166
-----	--	-----

FIGURE	PAGE
<p>8.2 Comparative TPR spectra of unpromoted 25%Co/Al₂O₃ catalyst (bottom) with metal promoted 25%Co/Al₂O₃ catalysts before and after simulated regeneration cycles, including (A) 1.0%Pt-25%Co/Al₂O₃, (B) 0.52%Ru-25%Co/Al₂O₃, (C) 0.95%Re-25%Co/Al₂O₃, (D) 0.55%Ag-25%Co/Al₂O₃, (E) 1.0%Au-25%Co/Al₂O₃, (F) 0.53%Rh-25%Co/Al₂O₃ (G) 0.99%Ir-25%Co/Al₂O₃, including after 1 cycle (RO1), 2 cycles (RO2), and 3 cycles (RO3).</p>	170
<p>8.3 Normalized XANES spectra at the Co K-edge of cobalt reference compounds compared to metal promoted 25%Co/Al₂O₃ catalysts before and after simulated regeneration cycles, including (A) 1.0%Pt-25%Co/Al₂O₃, (B) 0.52%Ru-25%Co/Al₂O₃, (C) 0.95%Re-25%Co/Al₂O₃, (D) 0.55%Ag-25%Co/Al₂O₃, (E) 1.0%Au-25%Co/Al₂O₃, (F) 0.53%Rh-25%Co/Al₂O₃, and (G) 0.99%Ir-25%Co/Al₂O₃, including after 1 cycle (Activated RO1) or 2 cycles (Activated RO2).</p>	173
 CHAPTER IX 	
<p>9.1 Comparative TPR spectra of unpromoted Co/Al₂O₃ catalysts. Pt promoted Co/Al₂O₃ catalysts, and Pt promoted Co/Calgon carbon catalyst.</p>	195
<p>9.2 Normalized XANES spectra of reference compounds.</p>	197
<p>9.3 Comparative normalized XANES spectra of (solid line) reduced sample and (dashed line) FTS sample of Pt-Co/Al₂O₃, Co/Al₂O₃, and Pt-Co/Calgon carbon catalysts.</p>	198
<p>9.4 The k¹-Weighted Fourier transform magnitude of Co K-edge EXAFS spectra of reference compounds, catalyst samples after reduction (solid line), and catalyst samples after</p>	

FIGURE	PAGE
exposure to the onset of the FTS conditions mimicking 50% CO conversion (dashed line).	199
9.5 The results of EXAFS fittings: (a) unfiltered k^1 -weighted $\chi(k)$ spectra; (b) filtered k^1 -weighted $\chi(k)$ spectra (solid line) and resulting of fitting (filled circles); (c) k^1 -weighted Fourier transform magnitude spectra (solid line) and resulting fitting (filled circles) over the first coordination shell of Co central atom, of (A) Co^0 foil reference and catalysts; (B) 0.5%Pt-5%Co/ Al_2O_3 , (C) 0.5%Pt-10%Co/ Al_2O_3 , (D) 10%Co/ Al_2O_3 , and (E) 0.5%Pt-2%Co/Calgon, at (I) after activation in H_2 and at (II) the onset of FTS at condition simulating 50% CO conversion.	204

APPENDIX

A1 Response area from GC FID as a function of injection volume of methane.	229
A2 Response area from GC FID as a function of injection volume of benzene.	230
A3 Response area from GC FID as a function of injection volume of toluene.	230
A4 Response area from GC FID as a function of injection volume of <i>p</i> -xylene.	231
A5 Response area from GC FID as a function of injection volume of <i>m</i> -xylene.	231
A6 Response area from GC FID as a function of injection volume of <i>o</i> -xylene.	232

ABBREVIATIONS

Ag	Silver
Ag _n ^{δ+}	Silver Cationic Cluster
Al ₂ O ₃	Aluminium Oxide or Alumina
ATR	Autothermal Reforming
Au	Gold
BET	Brunauer, Emmett, and Teller
C ₆ H ₆	Benzene
Calgon	Calgon Carbon
Car-	Carburized
CH ₄	Methane
Co	Cobalt
Co ₃ O ₄	Cobalt (II,III) oxide
CoAl ₂ O ₄	Cobalt Aluminate
CoO	Cobalt (II) oxide
CPO	Catalytic Partial Oxidation
EXAFS	Extended X-ray Absorption Fine Structure
F.C.C.	Faced Center Cubic
FID	Flame Ionization Detector
FT	Fischer-Tropsch
FTS	Fischer-Tropsch Synthesis
GTL	Gas-to-Liquids
H ⁺	Proton
Ir	Iridium
LC	Linear Combination (fitting)
Mo	Molybdenum
Mo ₂ C	Molybdenum Carbide
OR	Oxidation-reduction
Oxi-	Oxidized
Pt	Platinum
Re	Rhenium

Red-	Reduced
Rh	Rhodium
Ru	Ruthenium
SiO ₂	Silicon oxide or Silica
SMR	Steam Methane Reforming
TCD	Thermal Conductivity Detector
TPO	Temperature-Programmed Oxidation
TPR	Temperature-Programmed Reduction
TPR-EXAFS	Temperature Programmed Reduction- Extended X-ray Absorption Fine Structure
TPR-XANES	Temperature Programmed Reduction- X-ray Absorption Near Edge Structure
UV-Vis DRS	Ultraviolet-Visible Diffuse Reflectance Spectroscopy
WHSV	Weight Hourly Space Velocity
XANES	X-ray Absorption Near Edge Structure
XPS	X-ray Photoelectron Spectroscopy
XRD	X-ray Diffraction Spectroscopy
XRF	X-ray Fluorescence Spectroscopy

LIST OF SYMBOLS

\AA	Angstrom
B_d	Angle width of peak
D_h	Mean crystalline diameter
ΔH°_0	Standard enthalpy at reference conditions
ΔS°_0	Standard entropy at reference conditions
ΔG°_0	Standard Gibb free energy at reference conditions
K	Scherrer constant
λ	X-ray wavelength
θ	Bragg angle of the reflection (degree or radian)
K_a	The equilibrium constant
f_i	Fugacity of the species i
P	System pressure
T	System temperature
C_p	Heat capacity
ε	Extent of the reaction
S^2_0	The amplitude reduction factor
n_i	Fractional coordination
α	Isotropic expansion coefficient
σ^2	The Debye-Waller factor